Inorganic Chemistry

pubs.acs.org/IC Article

Silaiminyl-Silylene-Derived Unsymmetrical Diradicaloid Silacycles Isolated in Three Different Charge and Spin States

Chenfeng Wang,[▽] Yan Li,[▽] Sai Manoj N. V. T. Gorantla, Ming-Der Su,* Subuhan Ahamed, Zhifang Li,* Liviu Ungur,* and Kartik Chandra Mondal*

Cite This: *Inorg. Chem.* 2025, 64, 19961−19972 Read Online

ACCESS | Metrics & More | Article Recommendations | Supporting Information

ABSTRACT: Organosilicon diradicals with singlet or triplet spin states of the two unpaired electrons are one of the foci in main group chemistry. However, to date, the reported isolable ones are still scarce owing to their high reactivity and lack of suitable synthetic methods. In this article, a series of diradical silacycles and their corresponding isomers 1,3-disila-pyrroles were facilely obtained via the reactions of a silaiminyl-silylene (**1**) serving as a precursor of "masked" bis-silylene, with various diarylacetylenes. The computed reaction mechanisms indicated a concomitant and energetically favored formation of both isomers through distinct paths. Theoretical studies demonstrated that the singlet diradicaloid silacycles (**2**) bear two unpaired electrons asymmetrically distributed in the molecular backbone and have a remarkably small singlet−triplet energy gap that results in the observable NMR and electron paramagnetic resonance signals. Moreover, the reactivity studies of the diradical silacycle were also conducted, giving rise to multiple hydrochlorinated products under the treatment of HCl and a monoradical cation (**6**) and a dication (**7**) via stepwise oxidation of AgOTf. Compounds **6** and **7** were isolated, characterized, and studied by density functional theory calculations. Interestingly, the heterocyclic compound **4** containing a $CNPSi_2$ ring isolated from the reaction of **1** and Ad-C≡P showed Möbius-type aromaticity with the NICS(0) value of −6.8.

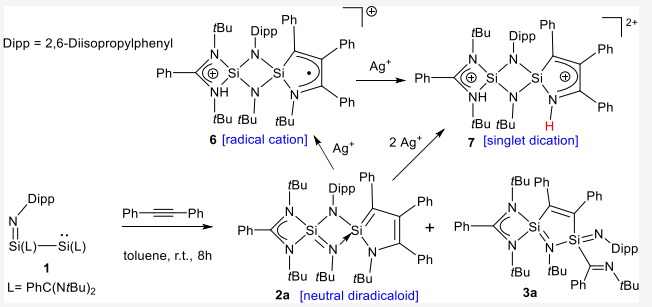

INTRODUCTION

Organosilicon radicals, acting as possible intermediates in many organic and metal organic reactions, have been at the forefront in current main group chemistry.[1−3] However, their high reactivity makes their synthesis formidable and challenging, and thus, this research field is still in its infancy.[4] Gomberg first synthesized a carbon-centered radical (Ph_3C) over a century ago. However, preparation and isolation of silicon-containing radicals are even more challenging.[1,2] Recently, progress has been made in the successful isolation of a series of organosilicon diradicals by taking advantage of amidinate-based silylenes[5,6] and cyclic alkyl (amino) carbenes (cAACs)[7] as effective ligands. The former has a rigid amidinate backbone with the Si(II) center being facilely functionalized, while the latter usually performs as a strong σ-donor and π-acceptor to harness the low-valent active metal or nonmetal centers.[6c,8]

The reaction of a bis(silylenyl)aniline with alkynes has been proven to be an effective strategy for constructing silacycles with a radical nature. By the reaction of bis-silylene LSi−SiL (L = $PhC(NtBu)_2$) with R−C≡C−R (R = Ph, TMS, and −C≡CTMS), the research groups of Roesky[5] and So[9] independently reported a six-membered cyclic $LSi(\mu_2\text{-}C_2R_2)_2SiL$ species as the congeners of 1,4-disilabenzenes with delocalized singlet diradical properties. Very recently, Driess et al. devised a series of novel 1,3-disila-pyrroles by reaction of a bis(silylenyl)aniline $(LSi)_2N\text{−}Ar'$ (L = $PhC(NtBu)$-2,4-tBu-$C_6H_4C(NtBu)_2$) with Ar−C≡C−Ar (Ar = Ph, 4-F-C_6H_4; Ar′ = Ph).[10a] Authors have reported the synthesis, isolation, and characterization of a spiro-diradical and its corresponding radical cation and dication (Scheme 1; top). Electron paramagnetic resonance (EPR) analysis and theoretical calculations showed the existence of asymmetric triplet diradicals, and the two unpaired electrons are mainly located on the two carbon atoms of the middle C_2NSi_2 ring and on the carbon atom of one amidinate−CN_2 chain, respectively. Their diradical nature was highlighted by the reactions with CCl_4 and AgOTf to give a double-chlorinated silane and stepwise one-electron oxidation derivatives, respectively. Two unpaired electrons are residing in two adjacent heterocyclic rings (Ar′ = Ph, Scheme 1; top). A completely different product (**2a**) was isolated by Roesky et al. when a similar reaction was carried out in Et_2O (Ar′ = Dipp, Scheme 1; bottom).[10b] The true identity of the electronic structure (zwitterionic singlet vs

Received: April 24, 2025
Revised: September 2, 2025
Accepted: September 11, 2025
Published: September 29, 2025

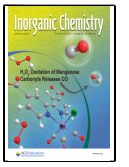

https://doi.org/10.1021/acs.inorgchem.5c01839
Inorg. Chem. 2025, 64, 19961−19972

Scheme 1. Previously Reported Triplet Diradical of 1,3-Disila-pyrroles (Top) and the Corresponding Singlet Zwitterionic Compound (Bottom) Obtained by Reaction of a Bis(silylenyl)aniline $(LSi)_2NPh$ (L = PhC(N*t*Bu)-2,4-*t*Bu-$C_6H_4C(N$*t*$Bu)_2$) with Ar−C≡C−Ar (Ar = Ph, 4-F-C_6H_4)

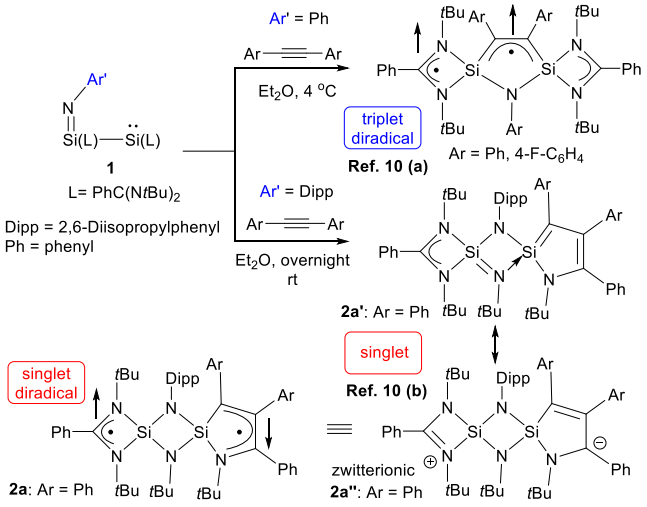

singlet diradical) of **2a** has not yet settled. Roesky et al. have represented **2a** as a singlet zwitterion (**2a′** and **2a″**; Scheme 1)[10b] based on natural resonance theory (NRT) calculations.[10cd−e] It is worth to mention that authors did neither perform CASSCF calculation nor looked for multireference character.[10b] Another important type of organosilicon diradicals is achieved on the basis of cAACs, such as $cAAC_2SiR_2$ (R = H and Cl) and cAAC-SiR_2-SiR_2-cAAC (R = Cl and Me), where the two unpaired electrons are mainly localized on the carbene carbon atoms. Among them, $(cAAC^{\bullet})_2SiCl_2$ should be singled out for its outstanding electronic structure.[6c] Theoretical calculations showed that it has a small singlet−triplet energy gap (ca. 4 kcal/mol), i.e., an amenable transition between the singlet diradical (diamagnetic) and triplet diradical (paramagnetic) at room temperature, which was confirmed by the observable NMR and EPR signals.[6c] It is worth noting that one of the advancements in the development of organosilicon diradicals has benefited from a stable N-linked bis-silylene $(LSi)_2NPh$ (L = amidinate ligand).[5,6,9,10a,b] There have been intensive documents on the idea that the bis-silylenes with different spacers can activate many small molecules through a Si(II)···Si(II) cooperative manner.[11]

In 2022, an improved synthesis of a silaiminyl-silylene LSi-Si(NDipp)L (L = $PhC(NtBu)_2$) (**1**), previously reported as a byproduct, was completed in the lab of Roesky.[12] They revealed that compound **1** can undergo unusual reversible electromerism between mono- and bis-silylenes. By density functional theory (DFT) calculations, **1** is only 2.15 kcal/mol more stable than the isomer bis-silylene LSi-N(Dipp)-SiL, while when the Dipp group is replaced by the Ph group, the corresponding bis-silylene form is considerably preferred by 12.67 kcal/mol relative to its silaiminyl-silylene form. Hence, the sterically demanding Dipp group on the nitrogen atom is inferred to be the cause of the chemical equilibrium between the mono- and bis-silylenes. In light of its exceptional electromerism property, **1** may act as a "masked" hemilabile bis-silylene ligand to apply in coordination chemistry. However, only some Cu(I) complexes using **1** as the ligand were reported in the literature hitherto.[12] Herein, we present a series of novel diradical silacycles derived from the reactions of silaiminyl-silylene (**1**) with diarylacetylenes. Their electronic structures and formation mechanisms were studied by theoretical calculations, and the related reactivity studies were also conducted. We have isolated structurally very different diradicals, radical cations, and dications employing different functional groups of N atoms, although a similar synthetic strategy of Driess et al.[10a] was followed, highlighting the future scope of unusual reactivity of silaiminyl-silylene (**1**). Interestingly, we have isolated a mixture of products (**2** and **3**; Scheme 2) in toluene, while Roesky et al. reported the isolation of only one product (**2**) from Et_2O (Scheme 1).[10b]

RESULTS AND DISCUSSION

Precursor **1** was reacted with PhC≡CPh in toluene in a 1:1 molar ratio immediately leading to an intense brown suspension, and after workup, some amount of brown crystalline solids was formed from the concentrated reaction solution. A mixture of black rod-shaped crystals and orange plates was seen under a microscope, suggesting the formation of two different products, which can be then readily separated by taking advantage of their different solubility in *n*-hexane. After the precipitate was washed with *n*-hexane, compound **2a** (Figure 1) was separated as an insoluble substance, while the *n*-hexane-soluble eluent was further concentrated to obtain

Scheme 2. Synthesis of Compounds 2a−b, 3a−c, and 4

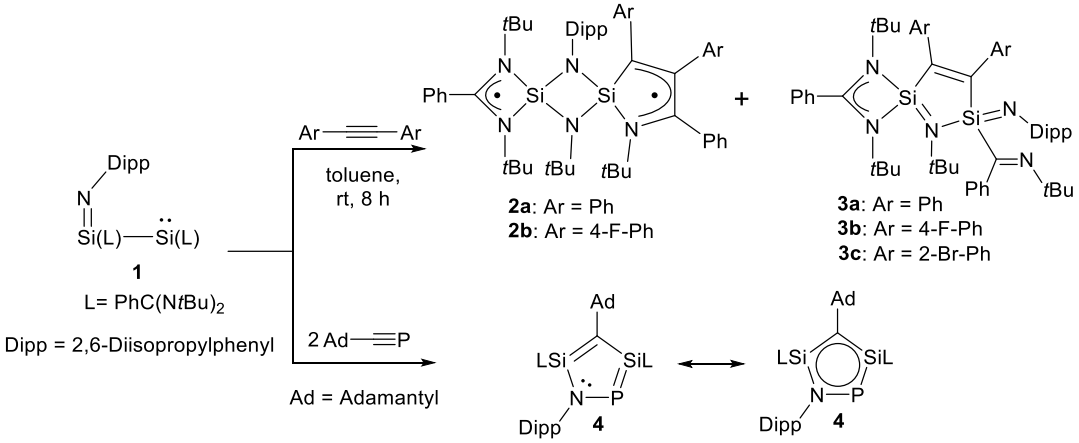

https://doi.org/10.1021/acs.inorgchem.5c01839
Inorg. Chem. 2025, 64, 19961−19972

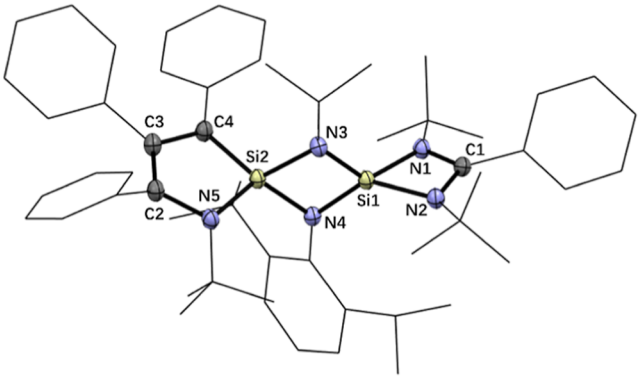

Figure 1. Molecular structure of neutral diradical **2a**. H atoms were omitted for clarity.

orange crystals of compound **3a**. Both products had almost the same yields of about 50% (Scheme 2). It is important to mention that Driess et al. have isolated a structurally different diradical in which the radical-containing heterocyclic rings are adjacent to each other as a single product (Ar′ = Ph).[10a] Roesky et al. have carried out a similar reaction between **1** and Ph_2C_2 in Et_2O, alike Driess et al, to isolate only compound **2a** (Ar′ = Dipp, Scheme 1).[10b]

In order to better understand the different reactivities of precursor silaiminyl-silylene (**1**) leading to the formation of compounds **2a** and **3a**, some test reactions were carried out in different molar ratios. However, the yielding ratios of the two products were always maintained at about 1:1, whether by changing the reaction temperatures (−30 to −60 °C) or the molar ratios of the starting materials or by using other solvents, such as Et_2O, THF, and DME. In addition, no interconversion between these two compounds (**2** and **3**) was found by simply heating their respective solutions. Similarly, compounds **2b** and **3b**/**3c** were obtained when different aryl groups were employed, showing a general trend of this reaction (Scheme 2). Therefore, it is reasonable to conceive that the two compounds were produced simultaneously through different reaction pathways. Compound **2a** is moderately soluble in toluene and is well soluble in THF, C_6H_5F, CH_2Cl_2, and MeCN. The ^{1}H NMR spectrum of **2a** in C_6D_6 shows four *t*-BuCH_3 signals at 1.87, 1.25, 1.15, and 0.90 ppm, indicative of the different chemical environments. The diagnostic resonance of Dipp−C*H* splits into two broad signals at 4.85 and 3.43 ppm, while the resonances of Dipp−CH_3 are partially coalesced with those of the *t*-Bu groups, which can be inferred from the integral areas. The ^{29}Si{H}NMR spectrum of **2a** shows two Si signals at −29.6 (*Si*N_4) and −50.5 (*Si*CN_3) ppm, which are typical Si(IV) signals with a significant shift relative to those (32.4 and −61.2 ppm) of **1**. Of particular interest is that diradical **2a** is not only NMR responsive but also EPR active.[10a]

The EPR spectrum of **2a** (measured in C_6D_6) exhibits a sharp signal at a g value of 2.02544 (see the Supporting Information), suggesting a paramagnetic property. Although the characteristic half-field transition signals for a triplet diradical were not observed even at ∼115 °C, the fact of observable NMR and EPR spectra can be detected indicates that **2a** may have a diradical nature, which is quite reminiscent of $(cAAC^{\bullet})_2SiCl_2$,[6c] a rare diradical species with a small singlet−triplet energy gap. The singlet-diradical state of **2** is responsible for clear NMR signals (see the Supporting Information), while the EPR spectra of **2** are due to the triplet-diradical as previously reported for $(cAAC^{\bullet})_2SiCl_2$.[6c]

The structural aspects of diradicals **2a** and **2b** are very similar and hence that of **2a** has been discussed here.[10b] The X-ray single-crystal diffraction studies showed that the structure of compound **2a** comprises a continuously linked three-ring system (Figure 1), i.e., a CN_2Si four-membered ring, an N_2Si_2 four-membered ring, and a C_3NSi five-membered ring (Figure 2). They are almost perpendicular to each other and are

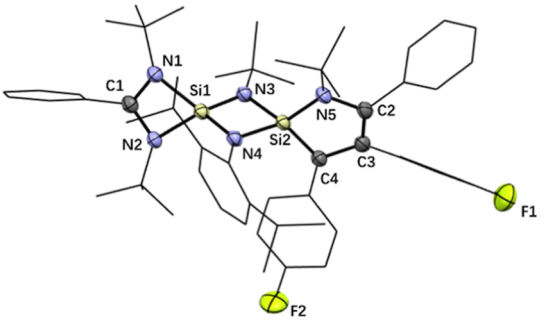

Figure 2. Molecular structure of neutral diradical **2b**. H atoms were omitted for clarity.

mutually connected by two tetra-coordinated Si atoms as the spiro centers, which is very different from that of the corresponding diradical isolated by Driess et al. (Scheme 1).[10a] Diradical **2** does not undergo oligomerization at room temperature (rt) in a cyclic manner unlike what has been observed by Driess et al.[10a] Two unpaired electrons in compound **2** are separated by the central four-membered ring (N_2Si_2), which may be the reason why **2** is stable as it is even at rt. The triplet diradical reported by Driess et al.[10a] is only stable at lower temperature (4 °C). Roesky et al. have shown that **2a** loses an alkene fragment when it is stirred for 3 days in Et_2O.[10b]

Both the amidinate CN_2Si and the central N_2Si_2 rings of **2a** exhibit virtually perfect planarity (the sums of the internal angles are 359.72° and 359.92°, respectively), while the C_3NSi ring is puckered with the N atom being slightly tilted with respect to the plane defined by C1−C2−C3.[10b] Three Ph groups are sited on the periphery of the C_3NSi ring. All the C atoms in the C_3NSi ring exhibit a trigonal planar configuration, and the C2−C3 (1.3755 Å) and C3−C4 (1.4501 Å) bond lengths lie between the typical C−C single and double bond lengths, signifying a conjugation of the C3-chain. These values are very close to those of C_2N and C_2Si_2N rings of the triplet diradical reported by Driess et al.[10a] The bond lengths of C1−N1 (1.3395 Å) and C1−N2 (1.3508 Å) in the amidinate ring of **2a** are comparable to those in monosilylenes LSi-Si(NDipp)L (1.345(3) Å and 1.340(3) Å).[13] The middle N_2Si_2 ring is trapezoidal with variable Si−N bond lengths (1.67−1.84 Å) that are still coherent with the range of Si−N single bonds.[10a] These observations suggest that the two radical electrons may be populated in the C3-chain of the C_3NSi ring and the CN_2 backbone of the amidinate ligand, respectively. It is notable that the bonding environment of the Si_2 atom in the C_3NSi ring features *S*-chirality, which is supported by a Flack parameter of less than 0.01. However, the circular dichroism (CD) optical rotation analysis revealed that **2a** has only a very small ee value of the *S*-enantiomer, and no

https://doi.org/10.1021/acs.inorgchem.5c01839
Inorg. Chem. 2025, 64, 19961−19972

R-enantiomer was actually isolated during the whole experiment.

Compared with **2a**, compound **3a** is soluble and stable in most aprotic solvents. **2a** produces the NMR signal due to the high population of the singlet diradical state alike the previously reported $(cAAC)_2SiCl_2$ diradical by Roesky et al.[6c] The $^{29}Si\{H\}NMR$ spectrum shows two Si signals at −25.9 ($SiCN_3$) and −78.1 (SiC_2N_2) ppm, demonstrating a Si(IV) character. X-ray crystallography showed that the structure of **3a** (Figure 3) can be described as a 1,3-disila-pyrrole

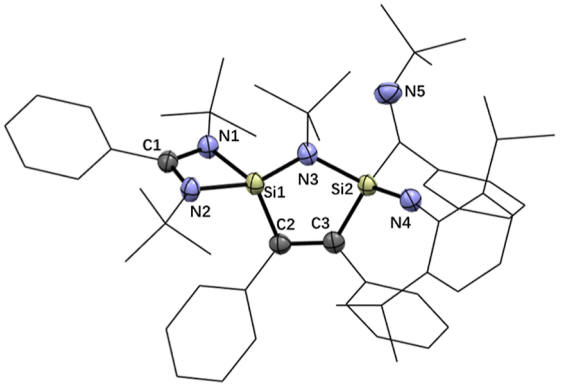

Figure 3. Molecular structure of neutral diradical **3a**. H atoms were omitted for clarity.

derivative, consisting of a slightly distorted C_2NSi_2 five-membered ring with two Si atoms bound by an intact and a broken amidinate ligand, respectively.

By employing a similar protocol, compounds **2b** and **3b** were prepared by the reaction of **1** with Ar−C≡C−Ar (Ar = 4-F-C_6H_4) in reasonable yields (45−50%). Compared to **2a**, the crystal structure of **2b** (Figure 2) has basically an identical backbone, but the Si atom of the C_3NSi five-membered ring exhibits *R*-chirality. It is worth noting that the F-Ph substituents on the periphery of the C_3NSi ring clearly point out the C≡C fragment arising from the alkyne substrate, which is not discernible in the structure of **2a** and is essential to comprehend the formation mechanism of **2a** (or **2b**). It should be emphasized that in contrast to the slow production of Driess' 1,3-disila-pyrrole diradicals (1−2 weeks for completing the reaction) that may be subjected to oligomerizations,[10a] the preparative reactions of compounds **2a** and **2b** proceeded much faster, and no free radical coupling was detected.

When Ar−C≡C−Ar (Ar = 2-Br-C_6H_4) was used instead of 1,2-diphenylethyne or 1,2-bis(4-fluorophenyl)ethyne, 1,3-disila-pyrrole **3c** was the sole product in 68% isolated yield, which is akin to that of **3a** and **3b** (Scheme 2). Further attempts by reacting various terminal alkynes Ar−C≡CH (Ar = ph, 2-F-C_6H_4-, 4-*i*Pr−C_6H_4) with **1** showed no reaction, as confirmed by ^1H NMR analysis. All of these results implied that the reaction chemistry of **1** and alkynes is not trivial.

To shed light on the formation mechanism of representative compounds **2a** and **3a**, DFT calculations were performed at the B3LYP-D3(BJ)/def2-SVP level of theory. The formation energy diagram of **2a** is shown in Figure 4. At the beginning of the reaction, by acquiring 16.4 kcal/mol energy from the environment, **1** interacts with Ph−C≡C−Ph to reach transition state **TS1A** that then transforms into intermediate **Int1A**. Subsequently, this intermediate surmounts an energy

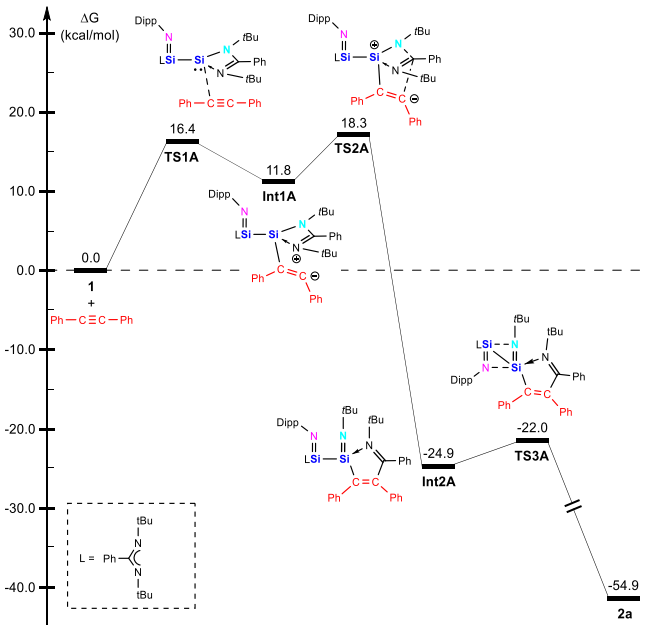

Figure 4. Free energy profile for the formation of **2a** at the B3LYP-D3(BJ)/def2-SVP level of theory.

barrier of 6.5 kcal/mol to transition state **TS2A**, and intermediate **Int2A** is formed after releasing a substantial energy of 43.2 kcal/mol. In this step, a random cleavage of either of the two C−N bonds in the amidinate ligand as well as the incorporation of the alkyne unit into the newly generated C_3NSi five-membered ring dictates the stereochemical outcomes of the chiral Si atoms in the **2a** and **2b** structures. Eventually, **Int2A** undergoes a [2 + 2] cycloaddition to form an N_2Si_2 four-membered ring via an easy Si−Si single bond rotation by overcoming an energy barrier of only 2.9 kcal/mol (**TS3A**) to the final product **2a**. The formation mechanism of **3a** was also theoretically studied and is shown in Figure S4 (see the Supporting Information).

By inspecting and comparing the above two mechanisms, two key points should be noted: (i) both are totally exothermic with their respective highest energy barriers (18.3 and 17.1 kcal/mol) being acceptable for a spontaneous reaction at room temperature and (ii) **1** and alkynes may interact concurrently in two distinct ways to form intermediates **Int2** (**2a**) and **Int2** (**3a**), respectively. These are thought to be instrumental in facilely furnishing compounds **2a** and **3a** in virtually equal yields. On the other hand, the exclusive production of compound **3c** can be explained in a theoretical view by that the energy of **3−2C-TS2** (38.5 kcal/mol, in Figure S4, see SI) is obviously higher than that of **3−3C-TS1** (14.6 kcal/mol, in Figure S5), which may be attributed to the more steric congestion of the 2-Br-C_6H_4 substituent of the alkyne substrate.

Considering the chemical similarities between phosphaalkynes (C≡P) and alkynes (C≡C), the reaction of **1** with Ad-C≡P (Ad = adamantyl) was performed. A deep red solution was obtained by mixing **1** with Ad-C≡P in toluene in a molar ratio of 1:1, from which compound **4** was isolated as red crystals in 64% yields (Scheme 2). The $^{31}P\{H\}NMR$ spectrum of **4** shows a sharp singlet at 80.8 ppm, and the $^{29}Si\{H\}NMR$ spectrum shows two resonances at 37.6 ppm ($J_{Si,p}$ = 132.8 Hz) and 18.4 ppm, corresponding to the Si signals of Si = P and Si = C, respectively. X-ray crystallography showed that **4** can be

https://doi.org/10.1021/acs.inorgchem.5c01839
Inorg. Chem. 2025, 64, 19961−19972

regarded as a heavy analog of cyclopentadiene, which consists of a distorted $CNPSi_2$ five-membered ring with an N atom slightly tilted from the plane defined by Si = C−Si−P and a two-coordinate P atom (Figure 5).

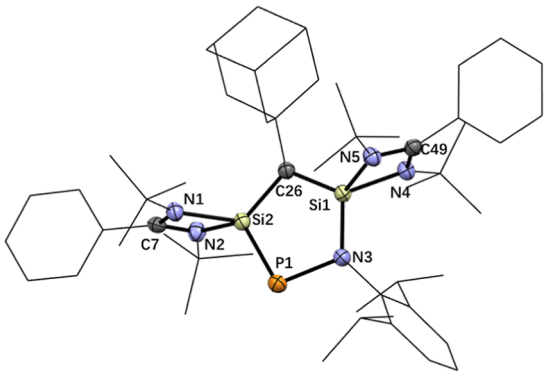

Figure 5. Molecular structure of **4**. H atoms are omitted for clarity.

The formation mechanism of **4** is not well understood, but it may undergo a complex incorporation of the C≡ moiety into the Si−Si = N fragment of **1**, which is referred to the formation of the silacycles derived from LSi-L′ (L = $PhC(NtBu)_2$, L′ = Cl and SiL) and R−C≡P (R = Me and Ad).[14] A series of experiments were conducted to explore the reactivity of compound **2a**. First, the treatment of **2a** with an excess of HCl (30 wt % in Et_2O) in toluene at room temperature afforded compound **5** as a white solid in 56% yields. The X-ray diffraction study showed a discrete structure of **5** as the result of a formal addition of HCl to **2a** in a 3:1 stoichiometry (Scheme 3). In the structure of **5** (Figure S2), a double-protonation and the dissociation of the L ligand lead to the formation of a separate $[LH_2]^+Cl^-$ fragment, while the remaining organic part features a double-chlorinated Si center

Scheme 3. Synthesis of Compounds 5−7

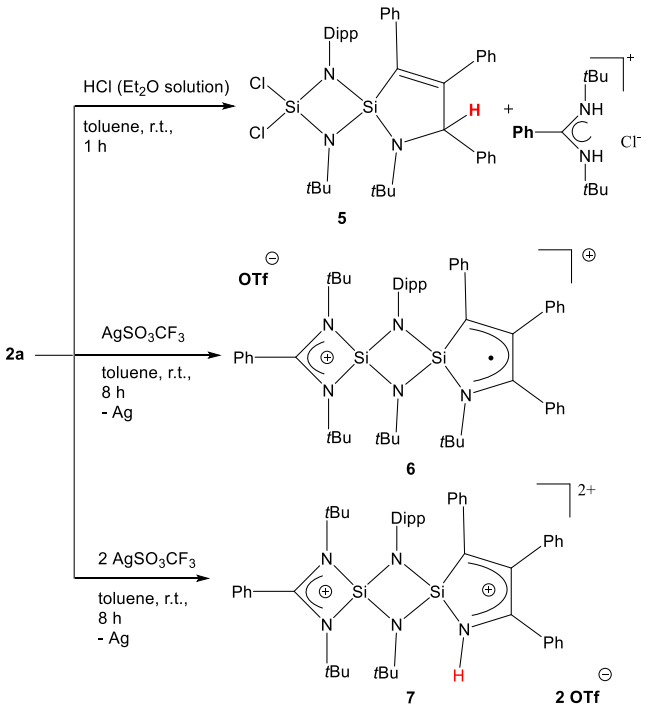

and a protonation of the C atom adjacent to the N atom in the C_3NSi ring.

This multiple hydrochlorination of **2a** may be facilitated by the two unpaired electrons residing on the amidinate backbone and the C_3NSi ring. The diradical nature of **2a** was further displayed by its stepwise oxidation of AgOTf. When **2a** was treated with one and two equivalents of AgOTf, black crystals of monoradical cation salt **6** (35% yields) and orange crystals of dication salt **7** (29% yields) were smoothly furnished, respectively (Scheme 3). X-ray crystallography showed that the molecular structures of neutral **2a**, radical monocation **6**, and dication **7** (Figure 6) are closely related in the main organic

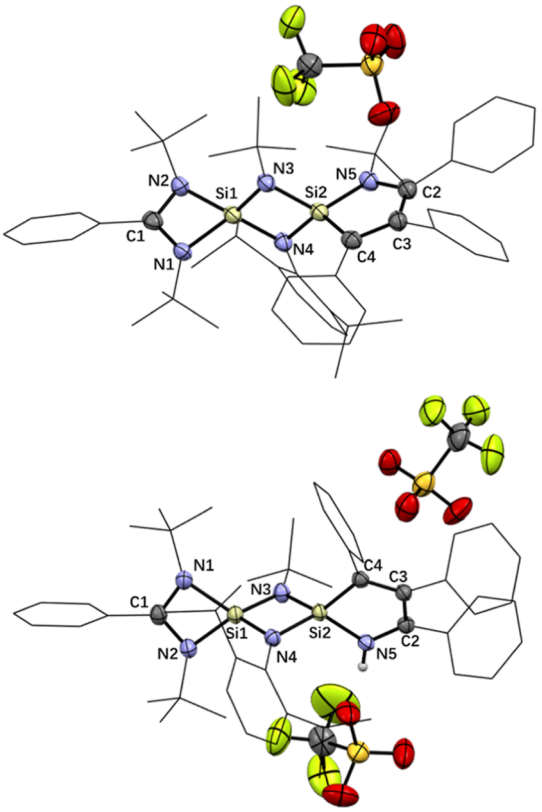

Figure 6. Molecular structures of monocation **6** (top) and dication **7** (bottom). H atoms are omitted for clarity.

parts. Unexpectedly, one *t*Bu group is replaced by an H atom in the C_3NSi ring of **7**, and the resulting NH moiety was confirmed by "H NMR" (a broad signal at 12.61 ppm) and IR ($\tilde{\nu}$ 3070 cm^{-1}) spectroscopy. The reason for this structural change is still unclear. Moreover, less obvious disparities were noticed by comparing the typical bond lengths of the amidinate CN_2Si rings and the C_3NSi rings in the structures of **2a** and **6** (Table 1). In contrast to the structural insensitivity of **2a** toward the one-electron oxidation to **6**, the bond lengths of N_5−C2 (1.308 Å) and C3−C4 (1.350 Å) in **7** are significantly shorter than those of **2a** (1.4508 and 1.4501 Å, respectively) and **6** (1.414 and 1.403 Å, respectively).[10a,b]

The calculated electron spin density diagrams clearly illustrate that one unpaired electron is delocalized over the C3-chain of the C_3NSi ring, which suggests that the radical electron on the amidinate CN_2-chain is more active upon AgOTf oxidation (Figure S8).

The optimized geometries of the neutral compound **2a** in its singlet state, the corresponding cationic compound **6** in the

https://doi.org/10.1021/acs.inorgchem.5c01839
Inorg. Chem. 2025, 64, 19961−19972

Table 1. Selected Bond Lengths (Å) in Compounds 2a, 5, and 6

bond	2a	5	6
C1−N1	1.351(2)	1.339(5)	1.345(4)
C1−N2	1.340(2)	1.351(5)	1.345(4)
N1−Si1	1.8030(10)	1.792(3)	1.805(3)
N2−Si1	1.8487(11)	1.829(3)	1.768(3)
Si1−N_3	1.6766(10)	1.692(3)	1.704(2)
Si1−N_4	1.7113(10)	1.715(3)	1.726(3)
Si_2−N_3	1.7939(10)	1.757(3)	1.725(3)
Si_2−N_4	1.8411(11)	1.787(3)	1.734(2)
Si_2−N_5	1.7499(10)	1.743(3)	1.782(2)
N_5−C2	1.451(2)	1.414(5)	1.308(4)
C2−C3	1.376(2)	1.412(6)	1.498(4)
C3−C4	1.450(2)	1.403(6)	1.350(4)
C4−Si_2	1.7945(13)	1.843(4)	1.857(3)

doublet state, and the dicationic compound **7** in the singlet state at the BP86-D3(BJ)/def2-TZVPP level and compound **2a** in the open-shell singlet diradical state at the UBP86-D3(BJ)/def2-TZVPP level of theory are shown in Figure S6. The computed bond lengths (Figure S6) in two spin states (singlet vs triplet, **2a**) are very close to each other and are slightly different than those of the experimental values (Table 1 and Figure S6). DFT calculations suggest that **2a** can have a singlet diradical ground state as well (Figure S8). The triplet diradical state of **2a** is slightly higher in energy than the closed-shell singlet state by 5.9 kcal/mol at the BP86-D3(BJ)/def2-TZVPP level of theory. Owing to the low energy differences between the different energy states, **2a** is expected to be in closed-shell singlet, open-shell singlet diradical and triplet diradical states in the solution, which is the reason why **2a** shows a strong EPR signal at $g \approx 2.0$ in the C_6D_6 solution (Figure S13, see the Supporting Information). However, further calculations considering B3LYP, M06-2X, PBE, and TPSS functionals with SVP and TZVP basis sets were carried out at the closed-shell singlet and triplet diradical states of **2a** (Table S6). The closed-shell singlet state of **2a** was found to be the ground state by ∼19−22 kcal/mol (SVP) and ∼20−23 (TZVP) with all four functionals mentioned above (Table S6, bottom). This energy difference can rationalize the sharp NMR signal of **2a** in solution alike a previously reported silicon(0) bridged 1,3-diradicaloid compound, $(cAAC^{\bullet})_2Si(0)$, of Roesky and Frenking et al.[6f] The energy difference between the closed-shell singlet and triplet states was reported to be ∼17−18 kcal/mol for the dark blue-colored diradicaloid compound $(cAAC^{\bullet})_2Si(0)$.[6f]

Mulliken spin densities reveal the spin densities in **2a**-triplet (as a minor conformer) (Figure S13) are distributed on C8 (0.49), C9 (0.39), and C11 (0.36), whereas the spin densities due to radical electron in cationic doublet compound **6** are delocalized on carbon 9 (0.40) and carbon 11 (0.31) atoms (Figures 7 and S7). **2a** is expected to be more stable in the closed-shell singlet or diradicaloid singlet state rather than in the triplet diradical state based on the computed energy difference. The computed g value of monoradical cation **6** is 2.002485 at the UB3LYP/6-311G(d,p) level of theory. The spin densities are mostly delocalized in the π-orbital of the C_3NSi ring of **6**. The C−C and N−Si−C units of the C_3NSi ring are found to accumulate the electron densities in **6**, which are in line with the EPR spectrum and the simulated hyperfine coupling constants (see the caption of Figure 7).

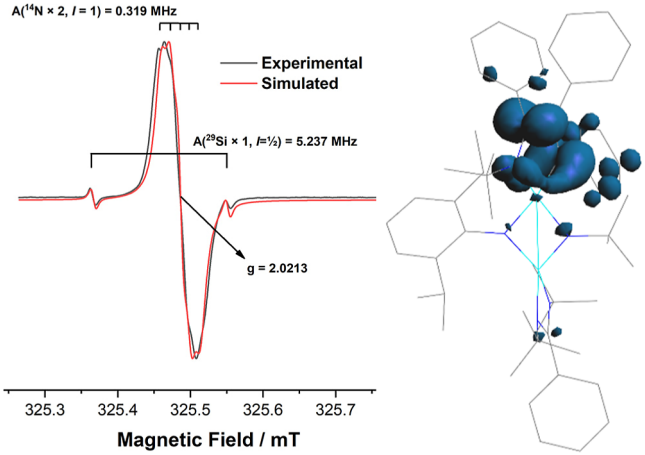

Figure 7. Red and black lines (left) represent the simulated (red) and the experimental (black) X-band EPR spectra of radical cation **6**. Fitting parameters using the EasySpin program. [g_{iso} = 2.0213, LWPP (Gaussian broadening) = 0.00444174 mT, LWPP (Lorentzian broadening) = 0.00479389 mT, $A(^{29}Si)$ = 5.24 MHz, $A(^{14}N)$ = 0.32 MHz, and X-band experimental frequency = 9.208205 GHz]. Mulliken spin densities of **6** (right) computed at the BP86-D3(BJ)/def2-TZVPP level of theory. Isodensity values at 0.003.

The Wiberg bond indices (WBI) from NBO calculations demonstrate the single-bond nature of the Si−N and Si−C bonds in compounds **2a**, **6**, and **7** (Table S2). The calculations further indicate significant charge polarization on the nitrogen atoms of Si−N bonds and on the carbon atom of the Si−C bond, which is supported by the high positive charge on the Si atoms and the negative charge on the bonded nitrogen and carbon atoms (Tables S2 and S3) eliminating any zwitterionic character (on two C-atoms of the alkyne unit) of **2a** with a very similar charge distribution in CN_2Si and C_2N_2Si rings (Figure 8). Roesky et al. have reported a singlet zwitterionic structure of **2a** (**2a′** and **2a″**; Scheme 1). They have carried out the calculations in different levels of theory.[10b] This difference may be due to the multireference character of compound **2a**.

The electronic structure of **2a** inferred to be challenging due to the presence of a multireference character, bringing a limitation to the DFT calculations.[18−25] The zwitterionic structure of **2a** reported by Roesky et al.[10b] may not be the true electronic structure (Scheme 1; **2a′** and **2a″**), which has been concluded based on NRT calculations.[10cd−e] To have a better understanding of the electronic ground state, ab initio multiconfigurational calculations of CASSCF/NEVPT2 type were performed on the full molecular system **2a** and on a structurally reduced version of it, using several computational models in terms of active space size and basis set employed. The aim of this computational work was to reveal the singlet−triplet energy gap, the nature of the ground-state wave function, and its diradical character in **2a**. Table 3 presents the calculated energy gaps using the largest structural and computational approximations feasible for our computers. Other results are given in Tables S6−S9.

The singlet−triplet energy gap is very small when **2a** is a diradical. DFT may not correctly describe the multiconfigurational wave function of the diradical, particularly the singlet state. The singlet state is (up-down spin to down-up spin); thus, there are two Slater determinants describing the state, while DFT is a singly determinant wave function, and hence, it

https://doi.org/10.1021/acs.inorgchem.5c01839
Inorg. Chem. 2025, 64, 19961−19972

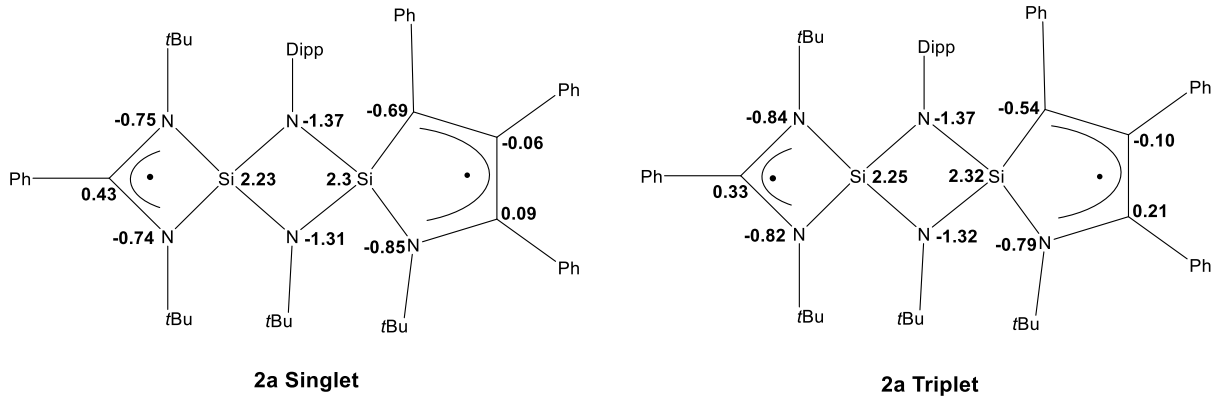

Figure 8. Natural charges on C, N, and Si atoms in nonradical singlet and triplet states of **2a** from NBO analysis at the BP86-D3(BJ)/def2-TZVPP level of theory.

Table 2. CASSCF/NEVPT2 Energy Gaps between the Ground Spin Open-Shell Diradical Singlet and the Lowest Spin Triplet in cm^{-1} [kcal/mol] Using the Full Molecular Structure of 2a, def2-TZVP Basis

	reduced structure		full structure
	CASSCF	NEVPT2	CASSCF
CAS(2 in 2)	186.1 [0.532]	394.6 [1.128]	157.2 [0.450]
CAS(4 in 4)	141.2 [0.404]	301.2 [0.861]	124.1 [0.355]
CAS(6 in 6)	143.1 [0.409]	291.3 [0.833]	124.1 [0.355]
CAS(8 in 8)	173.8 [0.497]	360.4 [1.030]	125.8 [0.360]
CAS(10 in 10)	188.9 [0.450]	380.2 [1.087]	124.0 [0.354]
CAS(12 in 12)	227.3 [0.650]	504.5 [1.442]	125.0 [0.357]
CAS(14 in 14)	215.4 [0.616]	479.1 [1.370]	125.2 [0.358]

Table 3. NICS Values of 3a and 4 at the BP86/def2-TZVPP Level of Theory

compound	3a	4	4-N-Me
NICS(0)	−2.428	−6.867	−7.669
NICS(1)	−1.700	−1.844	−3.466

can only describe one single determinant correctly. In the diradical case, the two electrons are not occupying the same molecular orbital, but rather they sit in different orbitals. This is the main difference from the closed-shell case where all electrons are paired. All calculations predict the ground state to be a spin singlet $S = 0$, while the spin triplet lies above, at a relatively small energy (Table 2). The singly occupied molecular orbitals are depicted in Figure 9. These multi-reference calculations yielded a CI vector with coefficients of 0.75 for the closed-shell (2,0) configuration and 0.66 for the (0,2) configuration. Therefore, compound **2a** is a closed-shell singlet species with a significant contribution from a doubly excited state, which imparts a singlet diradicaloid character. The corresponding values were reported to be 0.96 and 0.0 in (2,0) and (0,2) states, respectively, for the previously reported blue-colored silicon(0) bridged 1,3-diradicaloid compound $(cAAC^{\bullet})_2Si(0)$ of Roesky and Frenking et al.[6f] In this regard, the singlet diradical index proposed by Neese and co-workers[18a,b] can be calculated for an ab initio CI calculation using the canonical MOs by the following equation:

$$d = 200\sqrt{\frac{c_0^2 c_d^2}{c_0^2 + c_d^2}}$$

where c_0^2 is the weight of the closed-shell configuration in the CI wave function and c_d^2 is the weight of the double excitation. According to our values, the diradicaloid character is >99% for **2a** for all computational models. Table S10 shows the numerical details of this evaluation. A similar method was applied for the blue-colored silicon(0) bridged 1,3-diradicaloid compound $(cAAC^{\bullet})_2Si(0)$ of Roesky and Frenking et al.[6f] Subsequently, the radical cationic doublet analogue of $(cAAC^{\bullet})_2Si(0)$ was isolated by So et al.[6g] A three-center-two-electron (3C-2e) π-bond in $C_{cAAC}-Si-C_{cAAC}$ was theoretically predicted from DFT calculation. The nature of the Si−C bond and the distributions of spin densities on the C−Si−C backbone of $(cAAC^{\bullet})_2Si(0)$ were further studied by Stalke et al. via experimental charge density analysis.[6h] The experimental results from charge density measurements by Stalke et al.[6h] were in accordance with the DFT prediction of Frenking et al.[6f]

It is worth noting that for larger active spaces, the electrons have more freedom to form various configurations, and such configurations acquire some weight in the CASSCF optimization, thus decreasing the weight of the pure configurations (2,0 and 0,2) discussed above and used for the derivation of the above equation. This means that the diradicaloid definition is too simplistic for the large active space, where many configurations contribute to the ground state.

An important conclusion from our multireference and CASSCF calculations is that **2a** possesses more than 99% singlet diradicaloid character. The antiferromagnetic coupling ($J_{rad-rad}$) has been computed to be in the range of −100 to

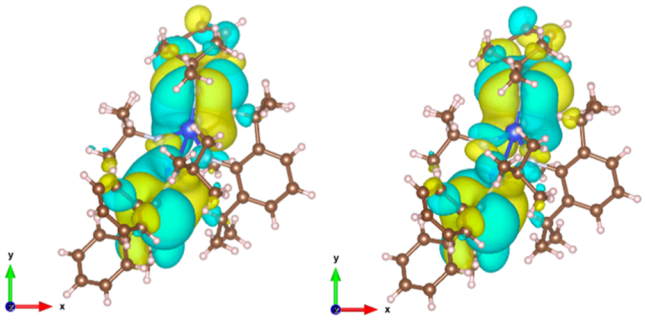

Figure 9. Singly occupied molecular orbitals of **2a** using the outcome of the TZVP basis, $S = 1$, full structure, CAS (14 el in 14 orbs). Orbitals #235 and #236.

https://doi.org/10.1021/acs.inorgchem.5c01839
Inorg. Chem. 2025, 64, 19961−19972

−500 cm^{-1}, which depends on the level of theory (see the Supporting Information). Thus, a tiny fraction of **2a** could be in triplet form, which gives a weak EPR signal. It is hard to get a forbidden transition at a measured temperature. A similar situation was found in $(cAAC^{\bullet})_2SiCl_2$.[6c]

The small energy gap between the closed-shell singlet and open-shell singlet diradical states of **2a** suggests that the molecule is likely to exist in both electronic states. **2a** shows an EPR single in C_6D_6 near $g \approx 2$.[1,6c] The signal became broad on cooling. Compound **2a** in the singlet electronic state is responsible for sharper NMR resonances, while the low-lying triplet state (5.9 kcal/mol) shows an EPR signal (Figure S13), which has been further correlated with the computation of Mulliken spin densities.[10a] Previously, $(cAAC^{\bullet})_2SiCl_2$ was shown to exit in both singlet (major) diradical and triplet diradical (minor) states.[6c] The singlet state of $(cAAC^{\bullet})_2SiCl_2$ showed a well-resolved NMR signal, while the minor conformer (triplet; less than 2%) produced an EPR signal.[1,6c]

Compound **2a** was found to be stable in C_6D_6 and also in CH_2Cl_2 (DCM), which was confirmed by recording EPR and NMR spectra. We have computed the transitions corresponding to UV−visible absorptions in a DCM solvent (SMD solvation model)[9] using the TD-DFT method. Compound **2a** shows three absorptions at wavelengths 511, 534, and 578 nm (Figure S10), depicting the transitions from the occupied delocalized electron cloud of silapyrrole (HOMO) to vacant π-type orbitals of the phenyl rings (LUMO + 6 to LUMO + 8).[6f] Similarly, the calculation suggests three absorptions for compound **6**, showing two transitions (468, 516 nm) from α-SOMO to α-LUMO + 3 and α-LUMO + 8 and one transition (629.6 nm) from β-SOMO to β-LUMO (Figure S11). The DFT computed wavelengths slightly differ from the experimental wavelengths, which is expected.

Additionally, we evaluated the aromatic character of the five-membered rings of compounds **3a** and **4** with Nuclear Independent Chemical Shift (NICS)[15] values (Table 3). NICS(1) is a suggested gauge of the π electron delocalization, whereas NICS(0) is considered as a measure of $\sigma + \pi$ electron delocalization.[16,17] Both **3a** and **4** demonstrated negative NICS values, indicating the aromatic character. However, compound **4** exhibited stronger aromaticity compared to that of **3a**, as indicated by more negative NICS values (Table S6). Interestingly, further evaluation of molecular orbitals in **3a** and **4** (Figures 10 and S12) unveiled Möbius topology with delocalized C−Si−N and Si−P π orbitals in opposite phases, suggesting the Möbius-type aromaticity (Figure 10)[16] due to the presence of heteroatoms in the five-membered ring. Further studies, by replacing Dipp with a Me group, revealed that the bulky Dipp group on the N atom of **4** reduces an aromatic character. The reported NICS(0) values of pyrrole and 1*H*-phosphole are −14.0 and −5.6, respectively, suggesting **4** is more aromatic than 1*H*-phosphole[17] but significantly less aromatic than pyrrole (Table 3).

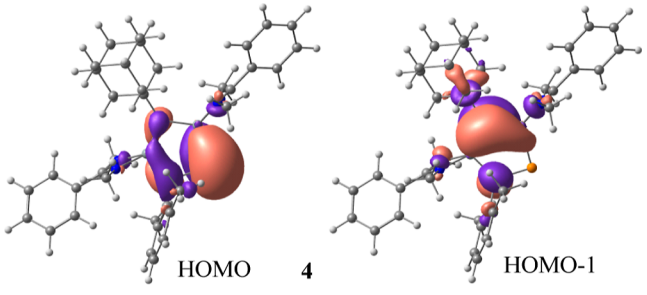

Figure 10. Molecular orbitals of compound **4** exhibiting Möbius topology. Isodensity values at 0.03.

CONCLUSIONS

In summary, two asymmetric spiro-silacycles **2a** and **2b** were synthesized via the reactions of a silaiminyl-silylene (**1**) with Ar−C≡C−Ar (Ar = Ph, 4-F-C_6H_4).[10b] In contrast, very difference final products (triplet spiro-diradical and corresponding spiro-radical cation and spiro-dication) were previously isolated and characterized from a chemical reaction between similar silaiminyl-silylene and alkyne by Driess et al.[10a] Theoretical studies showed the singlet diradicaloid nature of **2a**, with the two paired electrons being distributed on the amidinate CN2-chain and the C3-chain of the C_3NSi five-membered ring to give a closed-shell singlet electronic structure. In the same reaction system obtaining **2a** (or **2b**), 1,3-disila-pyrrole **3a** (or **3b**) was afforded as the second product in virtually equal yields with respect to **2a** (or **2b**) in Et_2O. Nevertheless, compound **3c** was the sole isolated product when varying the alkyne to more steric demanding Ar−C≡C−Ar (Ar = 2-Br-C_6H_4). Neutral compounds **2a** (or **2b**) and **3a** (or **3b**) are structural isomers, and theoretical calculations suggested that their formation proceeds spontaneously and concurrently at room temperature through distinct paths that are energetically favored, in accord with the equal isolated yields and the fact that no interconversion was observed between them. Isolation of these products was not reported from the reaction solution of toluene by Roesky et al.[10b] Comparatively, **1** reacted with phosphaalkyne Ad-C≡P to obtain exclusively product **4** featuring a $CNPSi_2$ five-membered ring, showing interesting Möbius-type aromaticity and completely different interaction modes between **1** and C≡C and C≡P bonds. Furthermore, the reaction of singlet diradicaloid **2a** with HCl (Et_2O solution) gave rise to compound **5** via multiple hydrochlorination and that with AgOTf furnished monoradical cation salt **6** and singlet dication **7** through stepwise one-electron oxidations. It is fascinating to isolate the same silicon compound in three different charge and spin states [neutral singlet diradicaloid (**2a**), cationic doublet (**6**), and dicationic singlet (**7**)]. In view of the remarkable electronic structure and reactivity of **1**, the great potential of it being applied as a precursor in coordination chemistry is envisioned. Finally, the electronic structure of **2a** was thoroughly studied here by computationally expensive multireferences and CASSCF calculations.[19−25]

EXPERIMENTAL SECTION

General Procedures. All key manipulations were carried out under a dry argon or nitrogen atmosphere by using Schlenk line and glovebox techniques. Toluene, THF, and hexane were dried by refluxing with sodium/potassium benzophenone under N_2. LSiCl was synthesized according to the literature.[12,13] ^1H, $^{13}C\{^1H\}$, $^{31}P\{^1H\}$, $^{29}Si\{^1H\}$, and $^{19}F\{^1H\}$ NMR spectra were recorded on a Bruker AVANCE II 400 or 500 spectrometer. Elemental analysis was performed on a Thermo Quest Italia SPA EA 1110 instrument. Commercial reagents were purchased from TCI and Sigma-Aldrich and were used directly.

Synthesis of 2a and 3a. At room temperature, to a mixture of **1** (0.69 g, 1.0 mmol) and PhC≡CPh (0.18 g, 1.0 mmol) was added toluene (30 mL), and the reaction mixture was stirred for 8 h. The resulting intense brown suspension was filtered, and the filtrate was concentrated under vacuum to 5 mL. After 2 days, a brown crystalline

https://doi.org/10.1021/acs.inorgchem.5c01839
Inorg. Chem. 2025, 64, 19961−19972

powder was deposited, which was washed by 2 × 5 mL of hexane to obtain **2a** as dark crystals. The hexane solution was concentrated to about 2 mL, where orange crystals of **3a** were grown.

2a: Yield: 51%. mp 170 °C (dec.). Elemental analysis calcd (%) for $C_{63}H_{81}N_5Si_2$ (964.50): C, 78.45; H, 8.46; N, 7.26. Anal. Found: C, 79.10; H, 8.19; N, 7.02. ^{1}H NMR (400 MHz, C_6D_6, 298 K, ppm): δ 7.81 (m, 1H, Ar*H*), 7.57 (m, 2H, Ar*H*), 7.31−6.62 (m, 20H, Ar*H*), 4.85 (br, 1H, C*H*Me$_2$), 3.43 (br, 1H, C*H*Me$_2$), 1.87 (s, 9H, NC*Me*$_3$), 1.75 (br, 3H, CH*Me*$_2$), 1.48−1.25 (m, 12H, CH*Me*$_2$ + NC*Me*$_3$), 1.25−1.15 (m, 12H, CH*Me*$_2$ + NC*Me*$_3$), 0.90 (s, 9H, NC*Me*$_3$), 0.84 (br, 3H, CH*Me*$_2$). ^{13}C{^{1}H} NMR (100 MHz, C_6D_6, 298 K, ppm): δ 180.9 (NCN), 152.8, 146.6, 145.1, 140.4, 137.8, 132.9, 131.5, 129.0, 128.5, 127.2, 127.0, 126.9, 126.0, 123.9, 123.4 (Ar*C* + *C*(Ph)), 56.8, 56.7, 54.9, 52.4 (CHMe$_2$ + NCMe$_3$), 34.5, 33.1, 31.4, 30.8, 29.9, 28.6, 28.3, 25.9, 25.5, 23.5 (CH*Me*$_2$ + NC*Me*$_3$). ^{29}Si{^{1}H} NMR (95 MHz, C_6D_6, 298 K, ppm): δ −29.6 (*Si*N$_4$), −50.2 (*Si*CN$_3$).

3a: Yield: 45%. mp 185 °C (dec.). Elemental analysis calcd (%) for $C_{63}H_{81}N_5Si_2$ (964.50): C, 78.45; H, 8.46; N, 7.26. Anal. Found: C, 78.28; H, 8.35; N, 7.32. ^{1}H NMR (400 MHz, C_6D_6, 298 K, ppm): δ 7.86 (d, 2H, Ar*H*), 7.42−7.36 (m, 6H, Ar*H*), 7.16−6.65 (m, 20H, Ar*H*), 4.01 (sept, 2H, J = 8 Hz, C*H*Me$_2$), 1.80 (s, 9H, NC*Me*$_3$), 1.49 (d, 6H, J = 8 Hz, CH*Me*$_2$), 1.36 (d, 6H, J = 8 Hz, CH*Me*$_2$), 1.15 (s, 18H, NC*Me*$_3$), 0.73 (s, 9H, NC*Me*$_3$). ^{13}C{^{1}H} NMR (100 MHz, C_6D_6, 298 K, ppm): δ 179.3, 178.8 (NCN + NCSi), 149.9, 145.8, 141.4, 141.3, 140.3, 137.5, 131.4, 131.2, 130.9, 129.0, 128.8, 128.5, 128.2, 128.0, 127.6, 127.1, 127.9, 126.4, 126.0, 125.3, 122.4, 112.6 (Ar*C* + *C*═*C*), 59.1, 55.7, 55.2, 54.5 (NCMe$_3$ + C*H*Me$_2$), 33.8, 31.8, 31.6, 30.4, 27.4, 26.0 (NC*Me*$_3$ + CH*Me*$_2$). ^{29}Si{^{1}H} NMR (95 MHz, C_6D_6, 298 K, ppm): δ −25.9 (*Si*CN$_3$), −78.1 (*Si*C$_2$N$_2$).

Synthesis of 2b and 3b. The synthetic procedure is similar to that of **2a** and **3a**, where ArC≡CAr (Ar = 4-F-C$_6$H$_4$; 0.21 g, 1.0 mmol) was employed.

2b: Yield: 52%. mp 195 °C (dec.). Elemental analysis calcd (%) for $C_{66}H_{83}F_2N_5Si_2$ (1046.55): C, 76.18; H, 8.04; N, 6.73. Anal. Found: C, 76.25; H, 7.97; N, 6.64. ^{1}H NMR (400 MHz, C_6D_6, 298 K, ppm): δ 7.54 (m, 3H, Ar*H*), 7.20−6.74 (m, 18H, Ar*H*), 4.72 (br, 1H, C*H*Me$_2$), 3.38 (br, 1H, C*H*Me$_2$), 1.82 (s, 9H, NC*Me*$_3$), 1.65 (br, 3H, CH*Me*$_2$), 1.47−1.25 (m, 12H, CH*Me*$_2$ + NC*Me*$_3$), 1.24−1.01 (m, 12H, CH*Me*$_2$ + NC*Me*$_3$), 0.98−0.66 (m, 12H, CH*Me*$_2$ + NC*Me*$_3$). ^{13}C{^{1}H} NMR (100 MHz, C_6D_6, 298 K, ppm): δ 186.8 (NCN), 162.6 (d, F-*Ph*, J_{Si-F} = 80.6 Hz), 160.7 (d, F-*Ph*, J_{Si-F} = 80.6 Hz), 158.2, 141.9, 134.3, 134.0 (d, F-*Ph*, J_{Si-F} = 3.3 Hz), 133.2, 132.2 (d, F-*Ph*, J_{Si-F} = 7.7 Hz), 132.0 (d, F-*Ph*, J_{Si-F} = 3.3 Hz), 129.9 (d, F-*Ph*, J_{Si-F} = 7.7 Hz), 129.7, 129.5, 129.4, 128.8, 128.7, 128.2, 126.8, 126.5, 125.7, 125.1, 115.6 (Ar*C* + N-*C*-*C*-*C*), 115.5 (d, F-*Ph*, J_{Si-F} = 21.5 Hz), 114.7 (d, F-*Ph*, J_{Si-F} = 21.5 Hz), 59.7, 58.8, 57.5, 54.8 (NCMe$_3$), 36.9, 35.0, 32.8, 31.8 (NC*Me*$_3$ + C*H*Me$_2$), 31.4, 31.0 (CH*Me*$_2$). ^{29}Si{^{1}H} NMR (95 MHz, C_6D_6, 298 K, ppm): δ −26.4(*Si*N$_4$), −46.5 (*Si*CN$_3$). ^{19}F{^{1}H} NMR (376 MHz, C_6D_6, 298 K, ppm): δ −119.8.

3b: Yield: 43%. mp 195 °C (dec.). ^{1}H NMR (400 MHz, C_6D_6, 298 K, ppm): δ 7.62 (m, 2H, Ar*H*), 7.45 (d, 2H, Ar*H*), 7.30−7.15 (br, 2H, Ar*H*), 7.03−6.53 (m, 15H, Ar*H*), 4.03 (sept, 2H, J = 8 Hz, C*H*Me$_2$), 1.79 (s, 9H, NC*Me*$_3$), 1.46 (d, 6H, J = 8 Hz, CH*Me*$_2$), 1.39 (d, 6H, J = 8 Hz, CH*Me*$_2$), 1.14 (s, 9H, NC*Me*$_3$), 1.13 (s, 9H, NC*Me*$_3$), 0.67 (s, 9H, NC*Me*$_3$). ^{13}C{^{1}H} NMR (100 MHz, C_6D_6, 298 K, ppm): δ 188.6 (NCN), 179.5, 175.5, 162.7 (d, F-*Ph*, J_{Si-F} = 41.7 Hz), 160.7 (d, F-*Ph*, J_{Si-F} = 41.7 Hz), 149.5, 149.6, 140.2, 137.2 (d, F-*Ph*, J_{Si-F} = 3.2 Hz), 136.8 (d, F-*Ph*, J_{Si-F} = 3.2 Hz), 133.0 (d, F-*Ph*, J_{Si-F} = 3.2 Hz), 131.2, 130.2 (d, F-*Ph*, J_{Si-F} = 3.2 Hz), 129.7, 128.2, 127.6, 127.1, 127.0, 126.6, 126.0, 122.6, 115.5 (d, F-*Ph*, J_{Si-F} = 21.2 Hz), 114.0 (d, F-*Ph*, J_{Si-F} = 21.2 Hz), 113.0 (Ar*C* + *C*═*C* + *C*═N), 59.2, 55.7, 55.1, 54.7 (NCMe$_3$), 33.9, 31.8, 31.5, 30.2, 27.4 (NC*Me*$_3$ + CHMe$_2$), 26.0, 25.9 (CH*Me*$_2$). ^{29}Si{^{1}H} NMR (95 MHz, C_6D_6, 298 K, ppm): δ −25.8 (*Si*CN$_3$), −79.2 (*Si*C$_2$N$_2$). ^{19}F{^{1}H} NMR (376 MHz, C_6D_6, 298 K, ppm): δ −115.1.

Synthesis of 3c. At room temperature, to a mixture of **1** (0.14 g, 0.2 mmol) and ArC≡CAr (Ar = 2-Br-C$_6$H$_4$; 0.067 g, 0.2 mmol) was added toluene (30 mL), and the reaction mixture was stirred for 8 h. The resulting intense red suspension was filtered, and the filtrate was concentrated under vacuum to 5 mL. Red crystals of **3c** were obtained. Yield: 0.15 g, 68%. mp 210 °C (dec.). Elemental analysis calcd (%) for $C_{63}H_{79}Br_2N_5Si_2$ (1121.31): C, 67.42; H, 7.10; N, 6.24. Anal. Found: C, 67.11; H, 7.18; N, 6.32. ^{1}H NMR (400 MHz, C_6D_6, 298 K, ppm): δ 8.86 (m, 1H, Ar*H*), 7.72 (m, 1H, Ar*H*), 7.55 (m, 3H, Ar*H*), 7.15−6.42 (m, 16H, Ar*H*), 4.54 (sept, 2H, J = 8 Hz, C*H*Me$_2$), 1.89 (s, 9H, NC*Me*$_3$), 1.65 (d, 6H, J = 8 Hz, CH*Me*$_2$), 1.60 (d, 6H, J = 8 Hz, CH*Me*$_2$), 1.42 (s, 9H, NC*Me*$_3$), 1.30 (s, 9H, NC*Me*$_3$), 0.65 (s, 9H, NC*Me*$_3$). ^{13}C{^{1}H} NMR (100 MHz, CD_3CN, 298 K, ppm): δ 186.2 (NCN), 181.0, 175.1, 149.4, 144.5, 143.1, 140.6, 137.6, 135.0, 133.9, 133.4, 131.9, 131.6, 130.7, 128.8, 128.4, 128.2, 128.1, 128.0, 127.2, 126.0, 125.9, 125.7, 125.1, 122.6, 121.3, 119.8, 111.4 (Ar*C* + *C*═*C* + *C*═N), 59.5, 56.5, 55.4, 55.0 (NCMe$_3$), 36.9, 34.5, 31.9, 31.3, 30.0 (NC*Me*$_3$ + CHMe$_2$), 26.4, 25.5 (CH*Me*$_2$). ^{29}Si{^{1}H} NMR (95 MHz, CD_3CN, 298 K, ppm): δ −25.1 (*Si*CN$_3$), −82.6 (*Si*C$_2$N$_2$).

Synthesis of 4. To a mixture of **1** (0.21 g, 0.30 mmol) and AdC≡P (0.055 g, 0.30 mmol) was added toluene (10 mL) at room temperature, and the reaction was stirred for 4 h. The resulted dark-red suspension was filtered, and the filtrate was concentrated under vacuum to 2 mL. Red crystals of **4** were grown at room temperature. Yield: 0.17 g, 64%. mp 200 °C (dec.). Elemental analysis calcd (%) for $C_{53}H_{78}N_5PSi_2$ (872.35): C, 72.97; H, 9.01; N, 8.03. Anal. Found: C, 72.51; H, 9.35; N, 7.75. ^{1}H NMR (400 MHz, C_6D_6, 298 K, ppm): δ 7.36−7.26 (m, 5H, Ar*H*), 7.01−6.85 (m, 8H, Ar*H*), 4.33 (m, 2H, C*H*Me$_2$), 2.56 (s, 5H, Ad*H*), 2.27 (s, 3H, Ad*H*), 2.10 (s, 2H, Ad*H*), 1.99 (m, 11H, Ad*H* + CH*Me*$_2$), 1.51 (m, 6H, CH*Me*$_2$), 1.44 (s, 18H, NC*Me*$_3$), 1.16 (s, 18H, NC*Me*$_3$). ^{13}C{^{1}H} NMR (100 MHz, C_6D_6, 298 K, ppm): δ 174.0, 172.0 (NCN), 148.8, 142.7, 137.5, 133.3, 131.8, 129.6, 129.0, 128.2, 126.8, 125.3, 123.8, 123.7, 122.9 (Ar*C* + SiC*C*Si), 54.4, 53.7, 48.6, 37.8, 37.0, 31.9, 31.8, 30.6, 27.9, 23.6 (Ad*C* + *C*HMe$_2$ + CH*Me*$_2$ + NCMe$_3$ + NC*Me*$_3$). ^{29}Si{^{1}H} NMR (95 MHz, C_6D_6, 298 K, ppm): δ 37.6 (d, $J_{P,Si}$ = 132.8 Hz, *Si*P), 18.4 (s, C*Si*N). ^{31}P{^{1}H} NMR (163 MHz, C_6D_6, 298 K, ppm): 80.8.

Synthesis of 5. At room temperature, to a toluene (15 mL) solution of **1** (0.087 g, 0.10 mmol) was added dropwise HCl (0.015 mL, 30 wt % Et$_2$O solution), and the reaction was stirred for 2 h. The resulting suspension was dried under vacuum to obtain a white powder, which was dissolved in a mixture of CH_2Cl_2/hexane (1:2, 2 mL). Colorless crystals of **5** were grown at 0 °C. Yield: 0.055 g, 56%. mp 245 °C (dec.). Elemental analysis calcd (%) for $C_{56}H_{76}Cl_3N_5Si_2$ (981.74): C, 68.51; H, 7.80; N, 7.13. Anal. Found: C, 68.22; H, 7.69; N, 7.22. ^{1}H NMR (400 MHz, $CDCl_3$, 298 K, ppm): δ 10.76 (s, 2H, N*H*), 7.83−6.90 (m, 23H, Ar*H*), 3.81 (m, 2H, C*H*Me$_2$), 3.59 (s, 1H, N−C*H*-C = C), 1.91 (m, 9H, NC*Me*$_3$), 1.36 (m, 27H, NC*Me*$_3$), 1.27 (m, 6H, CH*Me*$_2$), 0.97 (br, 6H, CH*Me*$_2$). ^{13}C{^{1}H} NMR (100 MHz, CD_3CN, 298 K, ppm): δ 167.6 (NCN), 164.0, 148.7, 148.4, 138.1, 138.0, 132.4, 131.8, 129.8, 129.1, 129.0, 128.8, 128.7, 128.6, 128.3, 128.1, 127.9, 127.5, 127.0, 126.7, 125.3, 124.0, 123.6 (Ar*C* + N-*C*-*C*═*C*), 58.4, 55.7, 55.3, 52.5 (NCMe$_3$ + N-*C*-*C*═*C*), 30.2, 30.1, 28.0, 27.8, 27.0, 22.7 (NC*Me*$_3$ + CHMe$_2$ + CH*Me*$_2$). ^{29}Si{^{1}H} NMR (95 MHz, CD_3CN, 298 K, ppm): δ −50.5 (*Si*CN$_3$), −71.1 (*Si*N$_2$Cl$_2$).

Synthesis of 6. At room temperature, to a mixture of **1** (0.087 g, 0.10 mmol) and $AgSO_3CF_3$ (0.026 g, 0.10 mmol) was added toluene (15 mL), and the reaction mixture was stirred for 8 h. The resulted brown suspension was filtered, and the insoluble solid was extracted with CH_2Cl_2 (10 mL). Black crystals of **5** were grown by slow evaporation of the solvent at room temperature. Yield: 0.042 g, 35%. mp 175 °C (dec.). Elemental analysis calcd (%) for $C_{59}H_{77}Cl_4F_3N_5O_3SSi_2$ (1191.29): C, 59.48; H, 6.52; N, 5.88. Anal. Found: C, 59.15; H, 6.60; N, 5.76.

Synthesis of 7. At room temperature, to a mixture of **1** (0.087 g, 0.10 mmol) and $AgSO_3CF_3$ (0.052 g, 0.20 mmol) was added toluene (15 mL), and the reaction mixture was stirred for 8 h. The resulted brown suspension was filtered, and the insoluble solid was extracted with CH_2Cl_2 (10 mL). Orange crystals of **7** were grown by slow evaporation of the solvent at room temperature. Yield: 0.067 g, 29%. mp 252 °C (dec.). Elemental analysis calcd (%) for $C_{109}H_{132}Cl_2F_{12}N_{10}O_{12}S_4Si_4$ (2313.74): C, 56.58; H, 5.75; N, 6.05. Anal. Found: C, 56.22; H, 5.60; N, 6.16. ^{1}H NMR (400 MHz, $CDCl_3$, 298 K, ppm): δ 12.61 (s, 1H, N*H*), 7.82−6.82 (m, 23H, Ar*H*), 3.28 (sept, 2H, J = 8 Hz, C*H*Me$_2$), 1.71 (s, 9H, NC*Me*$_3$), 1.32 (s, 18H,

https://doi.org/10.1021/acs.inorgchem.5c01839
Inorg. Chem. 2025, 64, 19961−19972

$NCMe_3$), 1.23 (s, 9H, $NCMe_3$), 1.21 (d, 6H, J = 8 Hz, $CHMe_2$), 1.16 (d, 6H, J = 8 Hz, $CHMe_2$). $^{13}C\{^1H\}$ NMR (100 MHz, $CDCl_3$, 298 K, ppm): δ 190.1, 189.5 (NCN + quaternary PhC), 152.3 (N-C−C-C), 152.1, 143.6, 139.2, 133.8, 132.9, 132.8, 132.0, 130.7, 130.0, 129.8, 129.6, 129.1, 128.2, 128.1, 127.5, 127.3, 126.6, 125.8, 125.3 (ArC), 124.8, 121.9, 119.4 (N−C-C-C + CF_3), 59.6, 58.7, 55.1 ($NCMe_3$), 33.4, 31.3, 31.0 ($NCMe_3$), 29.0 ($CHMe_2$), 27.4. 24.2 ($CHMe_2$). $^{29}Si\{^1H\}$ NMR (95 MHz, $CDCl_3$, 298 K, ppm): δ −27.8 (SiN_4), −45.6 ($SiCN_3$). $^{19}F\{^1H\}$ NMR (376 MHz, $CDCl_3$, 298 K, ppm): δ −78.1.

COMPUTATIONAL SECTION

Bonding Analysis and Transition State Calculations Details. See the Supporting Information and refs S3−S14.

Multiconfigurational Calculations with ORCA v6.0.1. Ab initio calculations for the Si_2-diradical system were performed with the ORCA 6.0.1 quantum chemistry package.[19] Two structural models were employed: the full molecule (Figure S14) and the reduced one (Figure S15), where *tert*-butyl and phenyl groups were replaced by methyl and hydrogen atoms, respectively. All atoms were described by the def2-SVP and def2-TZVP basis sets.[20] All calculations were accelerated by the resolution of identity (RI) methods, where all auxiliary density fitting basis sets were generated on the fly using the "AutoAux" generation procedure,[21] as implemented in ORCA.[22] An approximate second-order convergence method accelerated all DFT and CASSCF calculations.[23] Broken-symmetry DFT procedure was employed to find the magnetic exchange between the two radicals.[24] In this case, this method did not provide reasonable results. Similar untrustworthy results were obtained for the correct-spin DFT calculations, which is a true indicator of the multiconfigurational character of the ground state for this diradical system. Complete Active Space Self-Consistent Field calculations were performed to accurately estimate the singlet−triplet gap in the investigated system. Various sizes of active space were employed, ranging from the minimal CAS (2 in 2) to the largest feasible CAS (14 in 14).[18a] The *n*-electron valence second-order perturbation theory (NEVPT2) accounted for the dynamical electron correlation, as implemented in the ORCA package.[25]

ASSOCIATED CONTENT

Supporting Information

The Supporting Information is available free of charge at https://pubs.acs.org/doi/10.1021/acs.inorgchem.5c01839.

NMR, IR, EPR, coordinates, results from quantum chemical calculations, details of crystal structure refinement, and ^1H NMR spectra for all compounds (PDF)

Accession Codes

Deposition Numbers 2410295-2410302 contain the supplementary crystallographic data for this paper. These data can be obtained free of charge via the joint Cambridge Crystallographic Data Centre (CCDC) and Fachinformationszentrum Karlsruhe AccessStructuresservice.

AUTHOR INFORMATION

Corresponding Authors

Ming-Der Su − *Department of Applied Chemistry, National Chiayi University, Chiayi 60004, Taiwan; Department of Medicinal and Applied Chemistry, Kaohsiung Medical University, Kaohsiung 80708, Taiwan;* orcid.org/0000-0002-5847-4271; Email: midesu@mail.ncyu.edu.tw

Zhifang Li − *College of Material, Chemistry and Chemical Engineering, Key Laboratory of Organosilicon Chemistry and Material Technology, Ministry of Education, Hangzhou Normal University, Hangzhou 311121, China;* orcid.org/0000-0002-9548-2158; Email: zhifanglee@hznu.edu.cn

Kartik Chandra Mondal − *Department of Chemistry, Indian Institute of Technology Madras, Chennai 600036, India;* orcid.org/0000-0002-5830-3608; Email: chmlu@nus.edu.sg

Liviu Ungur − *Department of Chemistry, National University of Singapore, Singapore 119077, Singapore;* orcid.org/0000-0001-5015-4225; Email: csdkartik@iitm.ac.in

Authors

Chenfeng Wang − *College of Material, Chemistry and Chemical Engineering, Key Laboratory of Organosilicon Chemistry and Material Technology, Ministry of Education, Hangzhou Normal University, Hangzhou 311121, China*

Yan Li − *College of Material, Chemistry and Chemical Engineering, Key Laboratory of Organosilicon Chemistry and Material Technology, Ministry of Education, Hangzhou Normal University, Hangzhou 311121, China;* orcid.org/0000-0001-7703-6560

Sai Manoj N. V. T. Gorantla − *Department of Chemistry, Indian Institute of Technology Madras, Chennai 600036, India; Department of Chemistry, Hylleraas Center for Quantum Molecular Sciences, UiT The Arctic University of Norway, Tromsø N-9017, Norway;* orcid.org/0000-0001-7315-6354

Subuhan Ahamed − *Department of Chemistry, Indian Institute of Technology Madras, Chennai 600036, India*

Complete contact information is available at: https://pubs.acs.org/10.1021/acs.inorgchem.5c01839

Author Contributions

[▽]C.W. and Y.L. executed the experimental work and characterization, S.M.N.V.T.G. performed the bonding analysis. S.A. performed EPR simulation. M.-D.S. and Z.L. carried out the TS calculations. Y.L., M.-D.S., K.C.M., and Z.L conceived the fundamental scheme and supervised the study. L.U. has performed multiconfigurational calculations and also contributed to the main text. The manuscript has been written by Y.L., M.-D.S., K.C.M., L.U., and Z.L.

Notes

The authors declare no competing financial interest.

ACKNOWLEDGMENTS

This work is granted by the National Natural Science Foundation of China (Grant No. 22071039), the Zhejiang Provincial Natural Science Foundation (No. LY20B020009), and the Hangzhou leading innovation and entrepreneurship team project (TD2020015). K.C.M. thanks SERB, New Delhi (ECR/2016/000890), for funding and Senapathi Centre IIT M, Chennai, for computational facilities. Y.L. acknowledges the support from the Zhejiang Provincial University Leading Talents Program. M.-D.S. is grateful to the National Center for High-Performance Computing of Taiwan for generous amounts of computing time and to the Ministry of Science and Technology, Taiwan, for the financial support. K.C.M. thanks FIST grant for basic facilities at IIT Madras and computational facilities at IIT Madras, India. L.U. acknowledges the financial support of research projects A-8000709-00-

00, A-8000017-00-00, and A-8001894-00-00 of the National University of Singapore. Ab initio calculations were done on the ASPIRE-2A cluster (www.nscc.sg) under projects 11001278, 11003762, 51000267, and 11003763. This work used computational resources of the supercomputer Fugaku provided by RIKEN/NSCC through the HPCI System Research Project (Project ID: hp240202).

DEDICATION

This article is dedicated to Professor Herbert W. Roesky on the occasion of his 90th birthday.

REFERENCES

(1) (a) Chandra Mondal, K.; Roy, S.; Roesky, H. W. Silicon based radicals, radical ions, diradicals and diradicaloids. *Chem. Soc. Rev.* **2016**, *45*, 1080−1111. (b) Tumanskii, B.; Karni, M.; Apeloig, Y. Silicon-Centered Radicals. In *Organosilicon Compounds*; Lee, V. Y., Ed.; Academic Press, 2017; pp 231−294. (c) Power, P. P. Persistent and Stable Radicals of the Heavier Main Group Elements and Related Species. *Chem. Rev.* **2003**, *103*, 789−810. (d) Feng, Z. T.; Tang, S. X.; Su, Y. T.; Wang, X. P. Recent advances in stable main group element radicals: preparation and characterization. *Chem. Soc. Rev.* **2022**, *51*, 5930−5973.

(2) (a) Abe, M.; Ye, J.; Mishima, M. The chemistry of localized singlet 2. 1,3-diradicals (biradicals): from putative intermediates to persistent species and unusual molecules with a π-single bonded character. *Chem. Soc. Rev.* **2012**, *41*, 3808−3820. (b) Abe, M. Diradicals. *Chem. Rev.* **2013**, *113*, 7011−7088. (c) Kundu, S.; Sinhababu, S.; Chandrasekhar, V.; Roesky, H. W. Stable cyclic (alkyl)(amino)carbene (cAAC) radicals with main group substituents. *Chem. Sci.* **2019**, *10*, 4727−4741.

(3) (a) Zhang, X. P.; Fang, J. K.; Cai, C.; Lu, G. P. Recent advances in synthesis of organosilicons via radical strategies. *Chin. Chem. Lett.* **2021**, *32*, 1280−1292. (b) Ren, L. Q.; Li, N.; Ke, J.; He, C. Recent advances in photo- and electro-enabled radical silylation. *Org. Chem. Front.* **2022**, *9*, 6400−6415. (c) Wang, L.; Li, Y.; Li, Z.; Kira, M. Isolable silylenes and their diverse reactivity. *Coord. Chem. Rev.* **2022**, *457*, 214413. (d) Zhang, H. J.; Priebbenow, D. L.; Bolm, C. Acylsilanes: valuable organosilicon reagents in organic synthesis. *Chem. Soc. Rev.* **2013**, *42*, 8540−8571. (e) Davies, A. G. Organosilicon peroxides: radicals and rearrangements. *Tetrahedron* **2007**, *63*, 10385−10405.

(4) (a) Chen, X.; Gong, X. X.; Li, Z. Y.; Zhou, G.; Zhu, Z. H.; Zhang, W. L.; Liu, S. S.; Shen, X. Direct transfer of tri- and difluoroethanol units enabled by radical activation of organosilicon reagents. *Nat. Commun.* **2020**, *11*, 2756. (b) Kundu, S.; Samuel, P. P.; Sinhababu, S.; Luebben, A. V.; Dittrich, B.; Andrada, D. M.; Frenking, G.; Stueckl, A. C.; Schwederski, B.; Paretzki, A.; Kaim, W.; Roesky, H. W. Organosilicon Radicals with Si−H and Si−Me Bonds from Commodity Precursors. *J. Am. Chem. Soc.* **2017**, *139*, 11028−11031. (c) Otsuka, K.; Matsumoto, N.; Ishida, S.; Kyushin, S. An Isolable Radical Anion of an Organosilicon Cluster Containing Only σ Bonds. *Angew. Chem., Int. Ed.* **2015**, *54*, 7833−7836. (d) Nozawa, T.; Nagata, M.; Ichinohe, M.; Sekiguchi, A. Isolable p- and m-$[(tBu_2MeSi)_2Si]_2C_6H_4$: Disilaquinodimethane vs Triplet Bis(silyl radical). *J. Am. Chem. Soc.* **2011**, *133*, 5773−5775.

(5) Sen, S. S.; Roesky, H. W.; Meindl, K.; Stern, D.; Henn, J.; Stueckl, A. C.; Stalke, D. Synthesis, structure, and theoretical investigation of amidinato supported 1,4-disilabenzene. *Chem. Commun.* **2010**, *46*, 5873−5875.

(6) (a) Zhang, S. H.; Xi, H.; Lim, K. H.; So, C. W. Synthesis and Characterization of an Amidinate-Stabilized Siladithiocarboxylate and Its Germanium(II) Complex. *Organometallics* **2011**, *30*, 3686−3689. (b) Chen, Y.; Li, J.; Zhao, Y.; Zhang, L.; Tan, G.; Zhu, H.; Roesky, H. W. Stable Radical Cation and Dication of a 1,4-Disilabenzene. *J. Am. Chem. Soc.* **2021**, *143*, 2212−2216. (c) Mondal, K. C.; Roesky, H. W.; Schwarzer, M. C.; Frenking, G.; Tkach, I.; Wolf, H.; Kratzert, D.; Herbst-Irmer, R.; Niepötter, B.; Stalke, D. Conversion of a Singlet Silylene to a stable Biradical. *Angew. Chem., Int. Ed.* **2013**, *52*, 1801−1805. (d) Mondal, K. C.; Dittrich, B.; Maity, B.; Koley, D.; Roesky, H. W. Cyclic Alkyl(amino) Carbene Stabilized Biradical of Disilicontetrachloride. *J. Am. Chem. Soc.* **2014**, *136*, 9568−9571. (e) Kundu, S.; Samuel, P. P.; Sinhababu, S.; Luebben, A. V.; Dittrich, B.; Andrada, D. M.; Frenking, G.; Stueckl, A. C.; Schwederski, B.; Paretzki, A.; Kaim, W.; Roesky, H. W. Organosilicon Radicals with Si−H and Si−Me Bonds from Commodity Precursors. *J. Am. Chem. Soc.* **2017**, *139*, 11028−11031. (f) Mondal, K. C.; Roesky, H. W.; Schwarzer, M. C.; Frenking, G.; Niepötter, B.; Wolf, H.; Herbst-Irmer, R.; Stalke, D. A Stable Singlet Biradicaloid Siladicarbene: $(L:)_2Si$. *Angew. Chem., Int. Ed.* **2013**, *52*, 2963−2967. (g) Li, Y.; Chan, Y.-C.; Leong, B.-X.; Li, Y.; Richards, E.; Purushothaman, I.; De, S.; Parameswaran, P.; So, C.-W. Trapping a Silicon(I) Radical with Carbenes: A Cationic cAAC−Silicon(I) Radical and an NHC−Parent-Silyliumylidene Cation. *Angew. Chem., Int. Ed.* **2017**, *56*, 7573−7578. (h) Niepötter, B.; Herbst-Irmer, R.; Kratzert, D.; Samuel, P. P.; Mondal, K. C.; Roesky, H. W.; Jerabek, P.; Frenking, G.; Stalke, D. Experimental Charge Density Study of a Silylone. *Angew. Chem., Int. Ed.* **2014**, *53*, 2766−2770.

(7) (a) So, C. W.; Roesky, H. W.; Magull, J.; Oswald, R. B. Synthesis and Characterization of $[PhC(NtBu)_2]SiCl$: A Stable Monomeric Chlorosilylene. *Angew. Chem., Int. Ed.* **2006**, *45*, 3948−3950. (b) Sen, S. S.; Roesky, H. W.; Stern, D.; Henn, J.; Stalke, D. High Yield Access to Silylene RSiCl (R = $PhC(NtBu)_2$) and Its Reactivity toward Alkyne: Synthesis of Stable Disilacyclobutene. *J. Am. Chem. Soc.* **2010**, *132*, 1123−1126.

(8) Martin, D.; Soleilhavoup, M.; Bertrand, G. Stable singlet carbenes as mimics for transition metal centers. *Chem. Sci.* **2011**, *2*, 389−399.

(9) Yeong, H. X.; Xi, H. W.; Lim, K. H.; So, C. W. Synthesis and Characterization of an Amidinate-Stabilized cis-1,2-Disilylenylethene [cis-LSi{C(Ph)═C(H)}SiL] and a Singlet Delocalized Biradicaloid $[LSi(\mu_2\text{-}C_2Ph_2)_2SiL]$. *Chem.—Eur. J.* **2010**, *16*, 12956−12961.

(10) (a) Xiong, Y.; Dong, S.; Yao, S.; Lorent, C.; Krause, K. B.; Vijaykumar, G.; Zhu, J.; Limberg, C.; Driess, M. A class of non-aromatic 1,3-disilapyrroles acting as stable organosilicon-based triplet diradicals. *Nat. Synth.* **2023**, *2*, 678−687. (b) Jin, D.; Sun, X.; Hinz, A.; Roesky, P. W. Unconventional Insertions of Internal Alkynes into a Mixed-Valent Silaiminyl-Silylene. *Inorg. Chem.* **2024**, *63*, 18669−18675. (c) Glendening, E. D.; Landis, C. R.; Weinhold, F. NBO 7.0: New vistas in localized and delocalized chemical bonding theory. *J. Comput. Chem.* **2019**, *40*, 2234−2241. (d) Glendening, E. D.; Weinhold, F. Natural resonance theory: I. General formalism. *J. Comput. Chem.* **1998**, *19*, 593−609. (e) Glendening, E. D.; Weinhold, F. Natural resonance theory: II. Natural bond order and valency. *J. Comput. Chem.* **1998**, *19*, 610−627.

(11) (a) Maiti, A.; Stubbe, J.; Neuman, N. I.; Kalita, P.; Duari, P.; Schulzke, C.; Chandrasekhar, V.; Sarkar, B.; Jana, A. CAAC-Based Thiele and Schlenk Hydrocarbons. *Angew. Chem., Int. Ed.* **2020**, *59*, 6729−6734. (b) Maiti, A.; Chandra, S.; Sarkar, B.; Jana, A. Acyclic diaminocarbene-based Thiele, Chichibabin, and Müller hydrocarbons. *Chem. Sci.* **2020**, *11*, 11827−11833. (c) Nayak, M. K.; Sarkar, P.; Elvers, B. J.; Mehta, S.; Zhang, F.; Chrysochos, N.; Krummenacher, I.; Vijayakanth, T.; Narayanan, R. S.; Dolai, R.; Roy, B.; Malik, V.; Rawat, H.; Mondal, A.; Boomishankar, R.; Pati, S. K.; Braunschweig, H.; Schulzke, C.; Ravat, P.; Jana, A. A bis-NHC−CAAC dimer derived dicationic diradical. *Chem. Sci.* **2022**, *13*, 12533−12539.

(12) Yadav, R.; Sun, X.; Köppe, R.; Gamer, M. T.; Weigend, F.; Roesky, P. W. Stimuli Responsive Silylene: Electromerism Induced Reversible Switching Between Mono- and Bis-Silylene. *Angew. Chem., Int. Ed.* **2022**, *61*, 202211115.

(13) Zhang, S. H.; Xi, H. W.; Lim, K. H.; Meng, Q.; Huang, M. B.; So, C. W. Synthesis and Characterization of a Singlet Delocalized 2,4-Diimino-1,3-disilacyclobutanediyl and a Silylenylsilaimine. *Chem.—Eur. J.* **2012**, *18*, 4258−4263.

(14) (a) Sen, S. S.; Khan, S.; Roesky, H. W.; Kratzert, D.; Meindl, K.; Henn, J.; Stalke, D.; Demers, J. P.; Lange, A. Zwitterionic Si-C-Si-

https://doi.org/10.1021/acs.inorgchem.5c01839
Inorg. Chem. 2025, 64, 19961−19972

P and Si-P-Si-P Four-Membered Rings with Two-Coordinate Phosphorus Atoms. *Angew. Chem., Int. Ed.* **2011**, *50*, 2322−2325. (b) Sen, S. S.; Hey, J.; Eckhardt, M.; Herbst-Irmer, R.; Maedl, E.; Mata, R. A.; Roesky, H. W.; Scheer, M.; Stalke, D. A Stable Cation of a CSi_3P Five-Membered Ring with a Weakly Coordinating Chloride Anion. *Angew. Chem., Int. Ed.* **2011**, *50*, 12510−12513.

(15) (a) Schleyer, P. v. R.; Maerker, C.; Dransfeld, A.; Jiao, H.; van Eikema Hommes, N. J. R. Nucleus-Independent Chemical Shifts: A Simple and Efficient Aromaticity Probe. *J. Am. Chem. Soc.* **1996**, *118*, 6317−6318. (b) Chen, Z.; Wannere, C. S.; Corminboeuf, C.; Puchta, R.; Schleyer, P. v. R. Nucleus-Independent Chemical Shifts (NICS) as an Aromaticity Criterion. *Chem. Rev.* **2005**, *105*, 3842−3888.

(16) Cheung, L. F.; Kocheril, G. S.; Czekner, J.; Wang, L. S. Observation of Möbius Aromatic Planar Metallaborocycles. *J. Am. Chem. Soc.* **2020**, *142*, 3356−3360.

(17) (a) Duffy, M. P.; Delaunay, W.; Bouit, P. A.; Hissler, M. π-Conjugated phospholes and their incorporation into devices: components with a great deal of potential. *Chem. Soc. Rev.* **2016**, *45*, 5296−5310. (b) Baryshnikov, G. V.; Minaev, B. F.; Pittelkow, M.; Nielsen, C. B.; Salcedo, R. Nucleus-independent chemical shift criterion for aromaticity in π-extended tetraoxa[8]circulenes. *J. Mol. Model.* **2013**, *19*, 847. (c) Schleyer, P. v. R.; Manoharan, M.; Wang, Z.-X.; Kiran, B.; Jiao, H.; Puchta, R.; van Eikema Hommes, N. J. R. Dissected nucleus-independent chemical shift analysis of π-aromaticity and antiaromaticity. *Org. Lett.* **2001**, *3*, 2465−2468. (d) Schleyer, P. v. R.; Jiao, H.; Hommes, N. J. R. v. E.; Malkin, V. G.; Malkina, O. L. An evaluation of the aromaticity of inorganic rings: refined evidence from magnetic properties. *J. Am. Chem. Soc.* **1997**, *119*, 12669−12670.

(18) (a) Bachler, V.; Olbrich, G.; Neese, F.; Wieghardt, K. Theoretical Evidence for the Singlet Diradical Character of Square Planar Nickel Complexes Containing Two *o*-Semiquinonato Type Ligands. *Inorg. Chem.* **2002**, *41*, 4179−4193. (b) Herebian, D.; Bothe, E.; Neese, F.; Weyhermüller, T.; Wieghardt, K. Molecular and Electronic Structures of Bis-(*o*-diiminobenzosemiquinonato)metal(II) Complexes (Ni, Pd, Pt), Their Monocations and -Anions, and of Dimeric Dications Containing Weak Metal−Metal Bonds. *J. Am. Chem. Soc.* **2003**, *125*, 9116−9128.

(19) (a) Neese, F.; Wennmohs, F.; Becker, U.; Riplinger, C. The ORCA quantum chemistry program package. *J. Chem. Phys.* **2020**, *152* (22), 224108. (b) Neese, F. Software update: The ORCA program system—Version 5.0. *Wiley Interdiscip. Rev.:Comput. Mol. Sci.* **2022**, *12* (5), No. e1606.

(20) (a) Weigend, F.; Ahlrichs, R. Balanced basis sets of split valence, triple zeta valence and quadruple zeta valence quality for H to Rn: Design and assessment of accuracy. *Phys. Chem. Chem. Phys.* **2005**, *7* (18), 3297−3305. (b) Stoychev, G. L.; Auer, A. A.; Neese, F. Automatic Generation of Auxiliary Basis Sets. *J. Chem. Theory Comput.* **2017**, *13* (2), 554−562.

(21) (a) Izsak, R.; Hansen, A.; Neese, F. The resolution of identity and chain of spheres approximations for the LPNO-CCSD singles Fock term. *Mol. Phys.* **2012**, *110* (19−20), 2413−2417. (b) Izsak, R.; Neese, F. An overlap fitted chain of spheres exchange method. *J. Chem. Phys.* **2011**, *135* (14), 144105. (c) Izsak, R.; Neese, F. Speeding up spin-component-scaled third-order pertubation theory with the chain of spheres approximation: the COSX-SCS-MP3 method. *Mol. Phys.* **2013**, *111* (9−11), 1190−1195. (d) Neese, F. Approximate second-order SCF convergence for spin unrestricted wavefunctions. *Chem. Phys. Lett.* **2000**, *325* (1−3), 93−98.

(22) (a) Ginsberg, A. P. Magnetic exchange in transition metal complexes. 12. Calculation of cluster exchange coupling constants with the X.alpha.-scattered wave method. *J. Am. Chem. Soc.* **1980**, *102* (1), 111−117. (b) Noodleman, L. Valence bond description of antiferromagnetic coupling in transition metal dimers. *J. Chem. Phys.* **1981**, *74* (10), 5737−5743. (c) Noodleman, L.; Davidson, E. R. Ligand spin polarization and antiferromagnetic coupling in transition metal dimers. *Chem. Phys.* **1986**, *109* (1), 131−143. (d) Shoji, M.; Koizumi, K.; Kitagawa, Y.; Kawakami, T.; Yamanaka, S.; Okumura, M.; Yamaguchi, K. A general algorithm for calculation of Heisenberg exchange integrals J in multispin systems. *Chem. Phys. Lett.* **2006**, *432* (1−3), 343−347. (e) Soda, T.; Kitagawa, Y.; Onishi, T.; Takano, Y.; Shigeta, Y.; Nagao, H.; Yoshioka, Y.; Yamaguchi, K. Ab initio computations of effective exchange integrals for H−H, H−He−H and Mn2O2 complex: comparison of broken-symmetry approaches. *Chem. Phys. Lett.* **2000**, *319* (3), 223−230.

(23) (a) Kollmar, C.; Sivalingam, K.; Helmich-Paris, B.; Angeli, C.; Neese, F. A perturbation-based super-CI approach for the orbital optimization of a CASSCF wave function. *J. Comput. Chem.* **2019**, *40* (14), 1463−1470. (b) Kollmar, C.; Sivalingam, K.; Guo, Y.; Neese, F. An efficient implementation of the NEVPT2 and CASPT2 methods avoiding higher-order density matrices. *J. Chem. Phys.* **2021**, *155* (23), 234104. (c) Ugandi, M.; Roemelt, M. An Ab Initio Computational Study of Electronic and Structural Factors in the Isomerization of Donor−Acceptor Stenhouse Adducts. *J. Phys. Chem. A* **2020**, *124* (38), 7756−7767.

(24) (a) Guo, Y.; Sivalingam, K.; Kollmar, C.; Neese, F. Approximations of density matrices in N-electron valence state second-order perturbation theory (NEVPT2). II. The full rank NEVPT2 (FR-NEVPT2) formulation. *J. Chem. Phys.* **2021**, *154* (21), 214113. (b) Guo, Y.; Sivalingam, K.; Neese, F. Approximations of density matrices in N-electron valence state second-order perturbation theory (NEVPT2). I. Revisiting the NEVPT2 construction. *J. Chem. Phys.* **2021**, *154* (21), 214111. (c) Angeli, C.; Cimiraglia, R.; Cestari, M. A multireference n-electron Valence State Perturbation Theory study of the electronic spectrum of s-tetrazine. *Theor. Chem. Acc.* **2009**, *123* (3−4), 287−298.

(25) (a) Reference 18b. (b) Herebian, D.; Wieghardt, K. E.; Neese, F. Analysis and Interpretation of Metal-Radical Coupling in a Series of Square Planar Nickel Complexes: Correlated Ab Initio and Density Functional Investigation of [Ni(LISQ)2] (LISQ = 3,5-di-tert-butyl-o-diiminobenzosemiquinonate(1-)). *J. Am. Chem. Soc.* **2003**, *125*, 10997−11005. (c) Neese, F. Definition of corresponding orbitals and the diradical character in broken symmetry DFT calculations on spin coupled systems. *J. Phys. Chem. Solids* **2004**, *65*, 781−785.

https://doi.org/10.1021/acs.inorgchem.5c01839
Inorg. Chem. 2025, 64, 19961−19972